SANDIA REPORT
SAND20XX-XXXX
Printed Click to enter a date

Sandia National Laboratories

Estimation of the Attenuation Caused by Power Line Towers on an E1-HEMP Induced Excitation

Luis San Martin, Larry Warne

Prepared by
Sandia National Laboratories
Albuquerque, New Mexico
87185 and Livermore,
California 94550

Issued by Sandia National Laboratories, operated for the United States Department of Energy by National Technology & Engineering Solutions of Sandia, LLC.

Available to DOE and DOE contractors from
U.S. Department of Energy
Office of Scientific and Technical Information
P.O. Box 62
Oak Ridge, TN 37831

Telephone: (865) 576-8401
Facsimile: (865) 576-5728
E-Mail: reports@osti.gov
Online ordering: http://www.osti.gov/scitech

Available to the public from
U.S. Department of Commerce
National Technical Information Service
5301 Shawnee Rd
Alexandria, VA 22312

Telephone: (800) 553-6847
Facsimile: (703) 605-6900
E-Mail: orders@ntis.gov
Online order: https://classic.ntis.gov/help/order-methods/

ABSTRACT

In a transmission line, the coupling between a line and a tower above ground is evaluated when the excitation is an E1 high-altitude electromagnetic pulse (HEMP). The model focuses on capturing correctly the effect of the coupling on the peak of the HEMP induced current that propagates along the line. This assessment is necessary to accurately estimate the effect of the excitation on the systems and components of the power grid. This analysis is a step towards a quantitative evaluation of HEMP excitation on the power grid. The results obtained indicate that the effect can be significant, especially for lines heights of 20 meters or more.

ACKNOWLEDGEMENTS

The authors wish to thank the following individuals for their contributions

SNL Support

- Salvatore Campione
- Ross Guttromson
- Matthew Halligan

Reviewers

- Matthew Halligan
- Salvatore Campione

CONTENTS

LIST OF FIGURES

LIST OF TABLES

This page left blank

EXECUTIVE SUMMARY

The estimation of the excitation induced by an E1 high-altitude electromagnetic pulse (E1-HEMP) on a transmission line over ground is important to evaluate the effect of a E1-HEMP on the systems and equipment of the power grid. In this report, an estimation of the effect of coupling between a line, that could be part of the power transmission infrastructure and utility transmission lines, and a supporting tower, on the magnitude of an E1-HEMP induced excitation on the transmission line over conductive ground.

To bound this effect, the current induced on an infinite line when the incident field angle corresponds to the angle of maximum coupling to the transmission line is evaluated. This evaluation was carried out with our frequency domain telegrapher's equation solver ATLOG – Analytic Transmission Line Over Ground that has been previously verified. A Norton equivalent circuit is used to inject this current to evaluate the line-tower coupling effect on the induced current of the line over conductive ground. The effect of the line-tower coupling is represented by an impedance that has three parts: a capacitive part, that was estimated, and a tower characteristic impedance and a tower-footing resistance both of which were obtained from the literature. In the analysis for the estimation of the capacitance, it was found that most of the charge associated to the line-tower coupling is located near the point of minimum distance between the line and the tower. This was the justification to include a lump circuit element to represent this capacitance in the analysis of the attenuation induced by the line-tower-coupling.

The attenuation results induced by the line-tower coupling are compared with the attenuation induced by the losses in the ground to assess its relative importance. The results show that this effect can be significant, especially for line heights of 20 meters or more.

ACRONYMS AND DEFINITIONS

Abbreviation	Definition
ATLOG	Analytic Transmission Line Over Ground
CIGRE	The International Council on Large Electric Systems
EBB	Elementary Building Block
E1-HEMP	E1 High Altitude Electromagnetic Pulse
EM	Electromagnetic
FT	Fourier Transform
HEMP	High Altitude Electromagnetic Pulse
IFT	Inverse Fourier Transform
MIL-STD	Military Standard
PEC	Perfect Electric Conductor

1. INTRODUCTION

The estimation of the excitation induced by an E1-HEMP on a transmission line over ground is important to evaluate its effects on the systems and equipment connected to the power grid. The purpose of this study is to estimate the effect of the coupling between a line and a supporting tower on the magnitude of a E1-HEMP induced excitation on a transmission line over ground. To correctly bound this effect, the current induced on an infinite line when the incident field angle corresponds to the angle of maximum coupling to the transmission line is evaluated. In this report, an estimate of the attenuation of the E1-HEMP-generated excitation caused by the coupling to ground through the transmission line towers is presented.

The attenuation due to the presence of a tower is determined by the value of the impedance that couples that line to ground across the tower. Conductor lines in a transmission line are isolated from the towers by a distance that depends on the line-to-ground voltage. In this analysis, the coupling between a conductor line and ground through a tower is modeled as composed of three parts, a first capacitive part, coupling the conductor line and the metallic tower, and two additional impedances representing the tower characteristic impedance and the tower footing resistance, a contact resistance between the tower grounding and the soil. The approximate model of the coupling between a conductor line and ground through a tower considers these three parts connected in series. The analysis is focused on the attenuation of the maximum current of the propagating pulse induced by the E1-HEMP on the transmission line.

An analysis of the charge distribution on the line and the tower associated with the presence of the tower (i.e. changes of charge distribution with respect to the background charge distribution) shows that most of the charge is accumulated relatively close, here close means compared with the wavelength of the electromagnetic (EM) field, to the point of shortest distance between the line and the tower. This is the justification for the use of a lump capacitance in series with the tower and tower footing impedances in the model. The value of the capacitance was estimated from an analytical expression that was evaluated numerically. The evaluated capacitance together with the tower characteristic impedance and tower-footings resistance, obtained from the literature, were used to estimate the attenuation of the E1-HEMP-induced electromagnetic (EM) wave due to the towers.

Figure 1 shows a typical situation, with a line and the supporting towers. In the same figure, a circuit model is included, with the coupling to ground being represented by an impedance Z_{TOTAL}. The coupling impedance Z_{TOTAL} is made of contributions shown in Figure 2. In the model used, the total impedance Z_{TOTAL} is composed of three parts: a capacitance that couples the metallic tower and the line, the tower characteristic impedance and a resistance representing the tower footing resistance. The largest contribution to Z_{TOTAL} is the capacitance coupling between the line and the tower. Estimates of the value of this capacitance for various combinations of line and tower heights are included in the report.

The frequency domain model equations are solved with the telegrapher's equation solver ATLOG (Analytic Transmission Line Over Ground), to evaluate the current pulse induced by the E1-HEMP on an infinite line over ground. Initial contributions to the problem of a line over ground can

be found in [1], [2]. The exact solution of a filament above a conductive ground was provided in [3], [4]. For additional information about ATLOG see [5], [6], [7] and references therein, where ATLOG was developed and shown to provide results in good agreement with full-wave simulations.

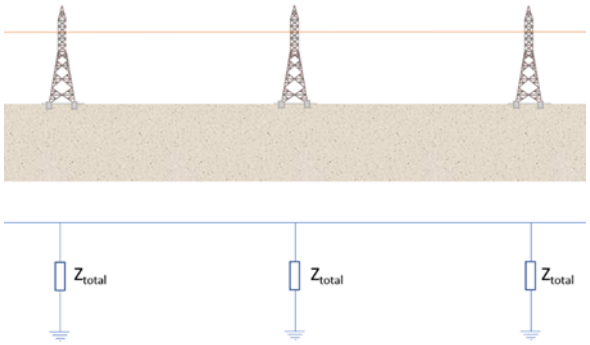

Figure 1: Typical situation of a line supported by towers and its circuit representation

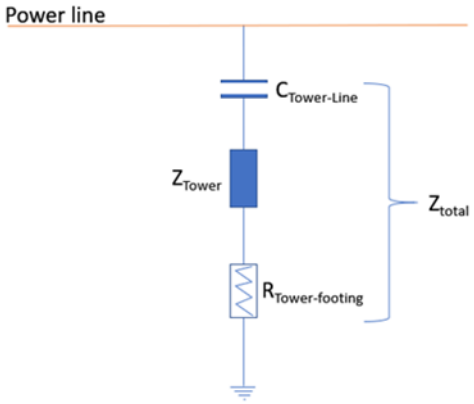

Figure 2: In our model, the total impedance is composed of three parts: a capacitance that couples the metallic tower and the line, the tower characteristic impedance and a resistance representing the tower footing resistance

Section 2 describes the E1-HEMP excitation of the transmission line and reviews the transmission line equations used in the analysis. The current induced on an infinite line is derived. This current is injected, with a Norton equivalent circuit, into a semi-infinite line, which without loss of generality can considered as starting at $z = 0$ and extending to infinity along the z positive direction, for the evaluation of the attenuation. Section 3 describes the procedure to evaluate the attenuation along the transmission line caused by the presence of the towers. A description of the analysis used to estimate the capacitive coupling between the conductor line and the metallic tower is given in Section 4. In this section, the capacitance values used in later sections are given. Section 5 gives the tower characteristic impedance and the footing resistance used in the analysis. In Section 6, the results for the attenuation due to the tower-line coupling are given, in table and graphic form, for several combinations of line and tower heights. Finally, conclusions are given in Section 7.

2. E1-HEMP ELECTROMAGNETIC EXCITATION AND TRANSMISSION LINE EQUATIONS

In the evaluation of the attenuation induced by the presence of the towers, the IEC61000-2-9 standard was used as E1-HEMP excitation. The pulse is given by the expression $E^{inc} = E_0 K(e^{-\alpha t} - e^{-\beta t})u(t)$ where the parameters are: $\alpha = 4x10^7 s^{-1}$, $\beta = 6x10^8 s^{-1}$, $E_0 = 50k\text{V/m}$ and $K = 1/(e^{-\alpha t_{\max}} - e^{\beta t_{\max}})$ with $t_{\max} = \log(\beta/\alpha)/(\beta - \alpha)$. This pulse is also known as the IEC-61000-2-9 [8]. In Figure 3, the pulse and its reconstruction via Fourier Transform (FT) and Inverse Fourier Transform (IFT) are shown.

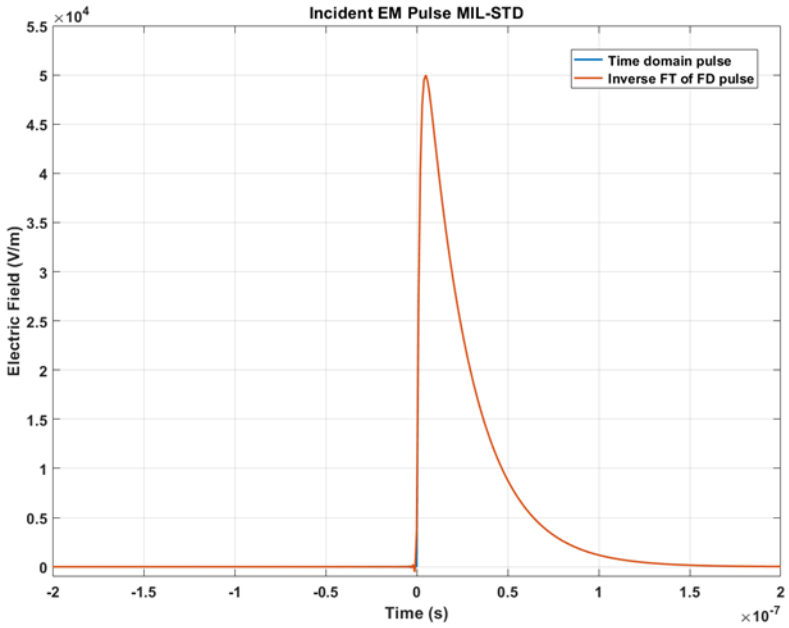

Figure 3: IEC61000-2-9 Pulse. Its width at half maximum is approximately 30 ns and the maximum value of the electric field is 50 KV/m

The frequency spectrum of the pulse in Fig. 3 is given in Figs. 4 and 5, for the magnitude and the phase of the IEC61000-2-9 pulse, respectively. These figures show the relevant part of the spectrum for the excitation pulse.

The analysis of the excitation of a transmission line over ground by a HEMP was reported in detail in [9]. Here, the parts of that analysis relevant to this work are included. In the transmission line equations, the different contributions to the transmission line parameters are given and the solution for the infinite line case is derived, which includes the attenuation due to the ground losses. The attenuation caused by the finite conductivity of the ground is a good reference to compare the attenuation caused by the towers, to assess its relative significance. Both results, i.e. attenuation with tower and without tower are included in the results of Section 6.

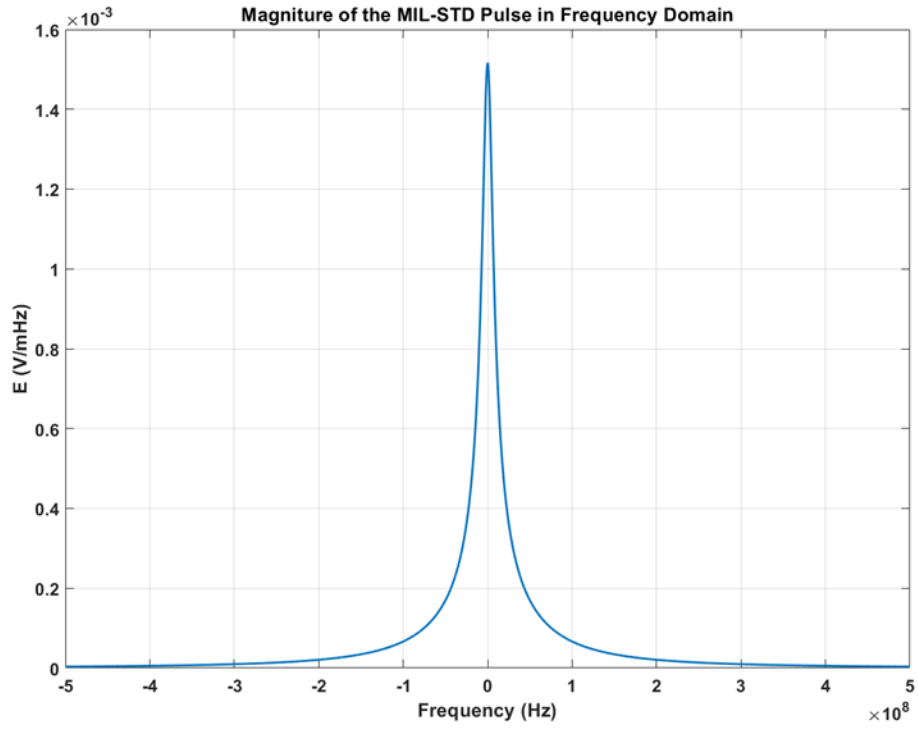

Figure 4: Frequency domain spectra of the magnitude of the MIL-STD pulse

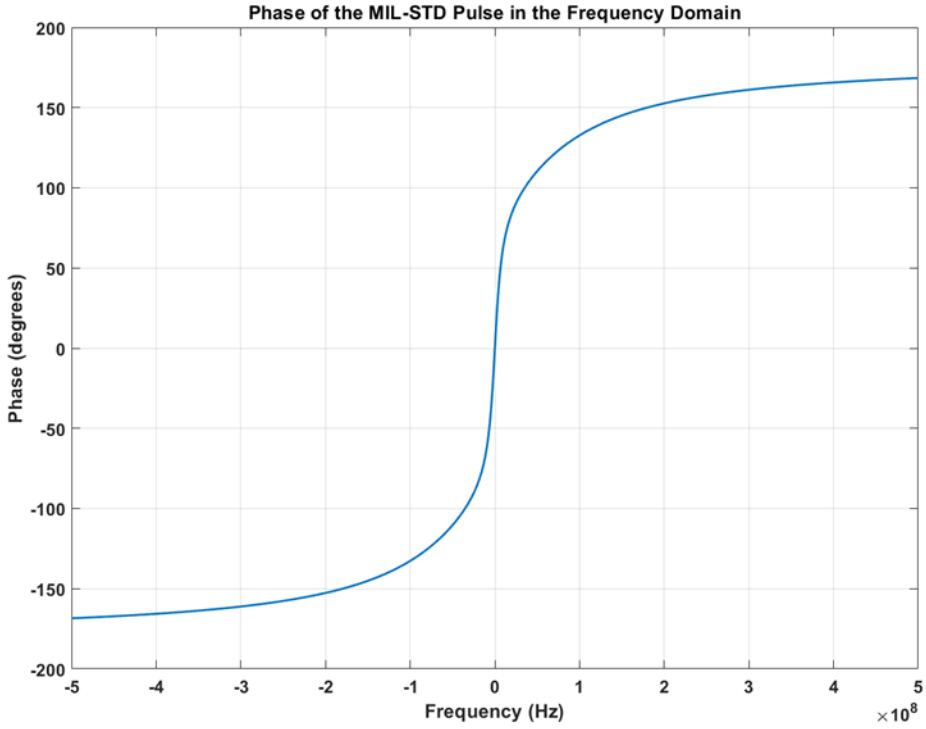

Figure 5: Frequency domain spectra of the phase of the MIL-STD pulse

The coupling of a HEMP to a transmission line mode is described here. Couplings to the vertical conducting paths, such as those that could be present on some of the loads connected to the line or to the tower itself are not considered in this report. A preliminary analysis of the vertical coupling to the towers obtained from a full wave simulation is presented in a separate report. The transmission line equations are:

$$\frac{dV}{dz} = -ZI + E_z^{inc}, \quad \frac{dI}{dz} = -YV \tag{1}$$

In equation (1) the impedance is defined as $Z = Z_0 + Z_2 + Z_4$. Here, focus is on the case of $h > b$ that applies to our case of interest (we take a $e^{j\omega t}$ time dependence), for additional details see [9].

$$Z_0 = \frac{\omega\mu_0}{2\pi}\frac{1}{(1-j)\frac{a}{\delta}} if \frac{\delta}{a} < \frac{1}{10}, \frac{j\omega\mu_0}{8\pi} + \frac{1}{\sigma_0\pi a^2} if \frac{\delta}{a} > 10, -\frac{j\omega\mu_0}{2\pi(1-j)\frac{a}{\delta}}\frac{J_0((1-j)\frac{a}{\delta})}{J_1((1-j)\frac{a}{\delta})} \text{ otherwise} \tag{2}$$

$$Z_2 = j\omega\frac{\mu_0}{2\pi}\ln(\frac{b}{a}) + j\omega\frac{\mu_0}{2\pi}\ln\left(\frac{h}{b} + \sqrt{\left(\frac{h}{b}\right)^2 - 1}\right) \; if \; h \geq b \tag{3}$$

$$Z_4 = j\omega\mu_0\frac{H_0^{(2)}(k_4 h)}{2\pi k_4 b H_1^{(2)}(k_4 h)} \quad if \; h \geq b \tag{4}$$

with $k_4^2 = \omega\mu_0(\omega\varepsilon_4 - j\sigma_4)$, $\delta = \sqrt{2/\omega\mu_0\sigma_0}$ and where ε_4 is the ground permittivity, σ_4 is the ground conductivity, σ_0 is the wire conductivity, a is the wire radius, b is the radius of the dielectric shell coating the wire, and h is the distance of the transmission line from the conducting ground plane. The admittance is defined as

$\frac{1}{Y} = \frac{1}{Y_e} + \frac{1}{Y_4}$ with $Y_e = j\omega C_e$ and

$$\frac{1}{C_e} = \sqrt{\left(\frac{h/h_e}{C_0} + \frac{1}{C_2}\right)^2 - \left(\frac{b/h_e}{C_0} + \frac{A_2}{C_2}\right)^2} \text{ if } h > b \tag{5}$$

where $h_e = \sqrt{h^2 - b^2}, C_2 = \frac{2\pi\varepsilon_0}{\ln(b/a)}$, and ε_2 is the permittivity of a dielectric shell coating the wire, A_2 given as $A_2 = 0.7\left(1 - \frac{a}{b}\right)\left(1 - \frac{h_e}{h}\right)\frac{(\varepsilon_2 - \varepsilon_0)}{(\varepsilon_2 + \varepsilon_0)}, C_0 = \frac{2\pi\varepsilon_0}{\ln\left(h/b + \sqrt{(h/b)^2 - 1}\right)}$, and the admittance Y_4 is given as

$$Y_4 = j\pi\left(\omega\varepsilon_4 - j\sigma_4\right)k_4 h\frac{H_1^{(2)}\left(k_4 h\right)}{H_0^{(2)}\left(k_4 h\right)} \;\; if \;\; h \geq b \tag{6}$$

We analyze the case of an infinite transmission line. By eliminating the voltage in Eq. (1)

$$\left(\frac{d}{dz} + k_L{}^2\right) I = -YE_z^{\;inc} \tag{7}$$

with $k_L = \sqrt{-ZY}$. The incident wave is assumed polarized in the plane containing the wire and perpendicular to the ground surface with incident angle θ_0 with respect to the z-axis, as depicted in Figure 6. Under this assumption the incident magnetic field for the case of a line above ground is

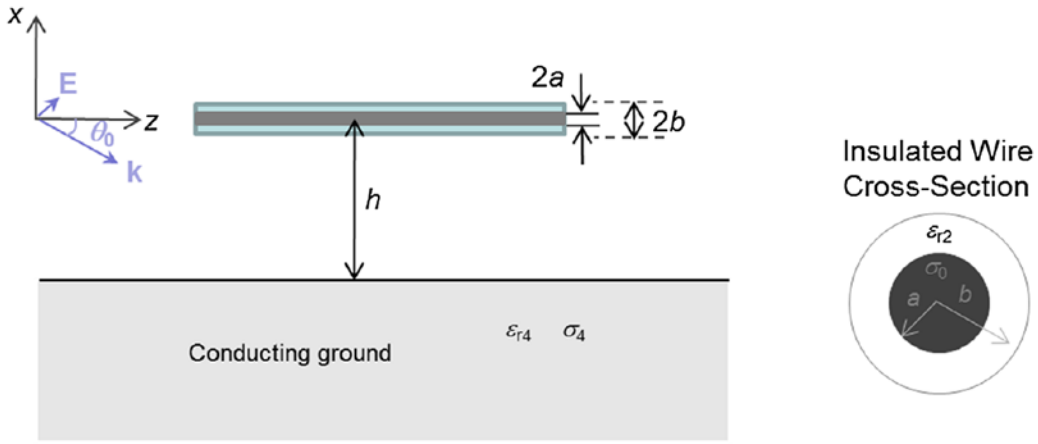

Figure 6: Schematic description of the incident wave direction on the transmission line indicating parameters of the problem

$$H_y^{\;inc} = \frac{1}{\eta_0}E_S(\omega)\left(e^{-jzk_0\cos\theta_0 + jxk_0\sin\theta_0} + R_H e^{-jzk_0\cos\theta_0 - jxk_0\sin\theta_0}\right) \;\; if \;\; x > 0 \tag{8}$$

T_H and R_H are the transmission and reflection coefficients and k_0 the free space wave number. In the case above ground it is convenient to set the phase reference on the wire itself at $z = 0$, which can be done by setting $E_S\left(\omega\right) = E\left(\omega\right)e^{-jhk_0\sin\theta_0}$, where $E\left(\omega\right)$ represents the spectrum of the incident HEMP.

$$E_Z^{\;inc} = \frac{1}{j\omega\varepsilon_0}\frac{dH_y^{\;inc}}{dx} = E_S\left(\omega\right)\sin\theta_0\left(e^{-jzk_0\cos\theta_0 + jxk_0\sin\theta_0} - R_H e^{-jzk_0\cos\theta_0 - jxk_0\sin\theta_0}\right) \; x > 0 \tag{9}$$

and $1 + R_H = T_H$, $1 - R_H = \dfrac{\sqrt{\left(k_4/k_0\right) - \cos^2\theta_0}}{\left(k_4/k_0\right)^2}T_H$, from where

$$R_H = \frac{(k_4/k_0)^2 \sin\theta_0 - \sqrt{(k_4/k_0)^2 - \cos^2\theta_0}}{(k_4/k_0)\sin\theta_0 + \sqrt{(k_4/k_0)^2 - \cos^2\theta_0}} \tag{10}$$

From the above expressions the incident electric field along the wire can be evaluated as

$$E_z^{inc} = E_S(\omega)\sin\theta_0 \left(e^{jhk_0\sin\theta_0} - R_H e^{-jhk_0\sin\theta_0}\right) e^{-jzk_0\cos\theta_0} = A_0 e^{-jzk_0\cos\theta_0} \quad h > 0 \tag{11}$$

By combining Eq. (11) and Eq. (7) the differential equation for the transmission line is

$$\left(\frac{d^2}{dz^2} + k_L{}^2\right) I = -YA_0 e^{-jzk_0\cos\theta_0} \tag{12}$$

whose general solution can be written as the sum of the particular solution and the homogeneous solution

$$I = C_1 e^{jk_L z} + C_2 e^{-jk_L z} - \frac{YA_0 e^{-jzk_0\cos\theta_0}}{k_L{}^2 - k_0{}^2\cos^2\theta_0} \tag{13}$$

which for the infinite wire, after dropping the homogeneous terms that blow up at $\pm\infty$, the solution is

$$I = -\frac{YA_0 e^{-jzk_0\cos\theta_0}}{k_L{}^2 - k_0{}^2\cos^2\theta_0} \tag{14}$$

To estimate the attenuation of the HEMP induced EM-wave on a transmission line caused by the towers, the current induced on a line of infinite length by the IEC61000-2-9 pulse described above is used. The line parameters used in the modeling are given as ground permittivity ε_4, with $\varepsilon_4 = 20\varepsilon_0$, ground conductivity $\sigma_4 = 0.01$ S/m and 0.001 S/m, wire radius $a = 1$ cm, with no insulation, wire conductivity $\sigma_0 = 2.9281\times10^7$ S/m and line height 10m, 20m, 30m and 40m. The current induced on an infinite line at $z = 0$, obtained from Eq. (14), is given by $I_i = -YA_0/\left(\Gamma^2 - k_0^2\cos^2\theta_0\right)$, with the angle of maximum coupling varying with height. This angle produces the largest current on the line for the given height. A matched Norton equivalent circuit is used, as was done in [10], to inject this current into a semi-infinite line for which the solution that satisfy the radiation condition as $z \to +\infty$ is

$$I = A_1 e^{i\Gamma z}, \qquad V = -i\Gamma\frac{A_1}{Y} e^{i\Gamma z}, \tag{15}$$

with $A_1 = 2I_i/\left(1 - i\Gamma Y_0/Y\right)$ and $Y_0 = \sqrt{Y/Z}$. This is done to use a typical pulse shape induced by the IEC61000-2-9 pulse on a transmission line in our evaluation of attenuation caused by the towers. The injected waveforms are shown in Figure 7 and Figure 8. The frequency content of the curves is given in Figure 9 and Figure 10. The angle of maximum coupling depends on the height of the line and the conductivity of the ground. The approximate angles of maximum coupling and the maximum currents induced at $z = 0$, on an infinite line for varying line-height and conductivity are given in Table 1. The selection of line heights corresponds to typical values as given in [11].

Table 1: Angles of Maximum Coupling and Currents for Varying Line Height and Ground Conductivity

Line Height, Conductivity	Maximum Current for Angle of Maximum Coupling	Angle of Maximum Coupling
[m], [S/m]	[A]	[Rad]
10, $\sigma = 0.01$	3546	$\theta = \pi / 33$
20, $\sigma = 0.01$	5350	$\theta = \pi / 49$
30, $\sigma = 0.01$	6676	$\theta = \pi / 57$
40, $\sigma = 0.01$	7760	$\theta = \pi / 64$
10, $\sigma = 0.001$	3403	$\theta = \pi / 34$
20, $\sigma = 0.001$	5008	$\theta = \pi / 45$
30, $\sigma = 0.001$	6176	$\theta = \pi / 53.5$
40, $\sigma = 0.001$	7106	$\theta = \pi / 61$

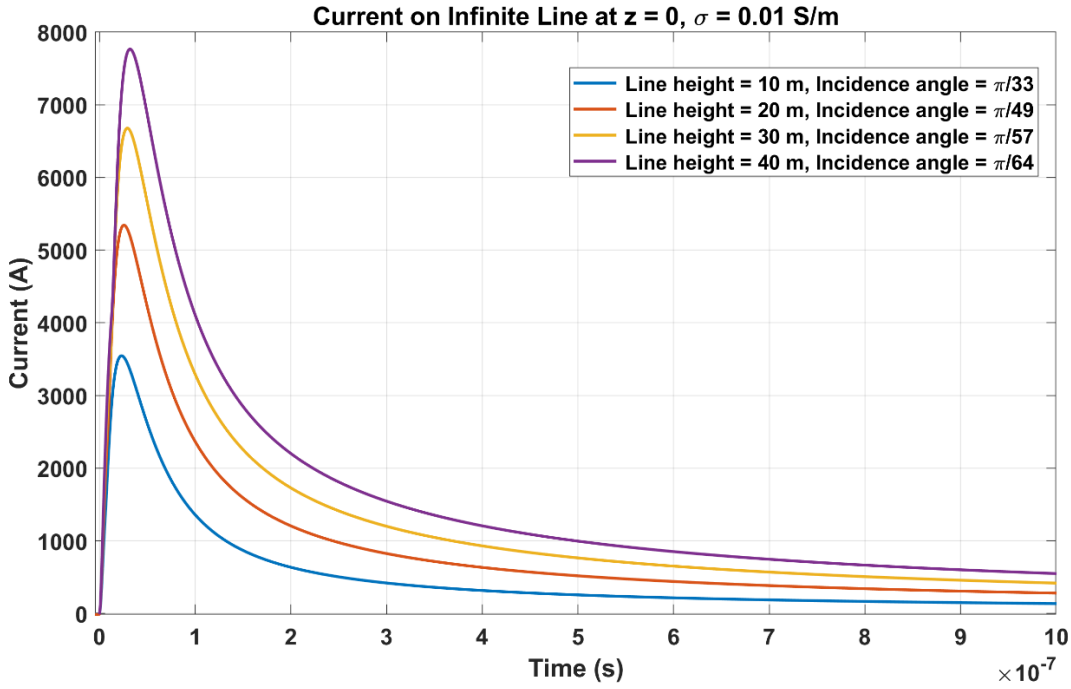

Figure 7: Time domain waveform of the current at z = 0 for the case of an infinite length line with a height of 10 m, 20 m, 30 m and 40 m, over ground with 0.01 S/m for incidence at angle of maximum coupling

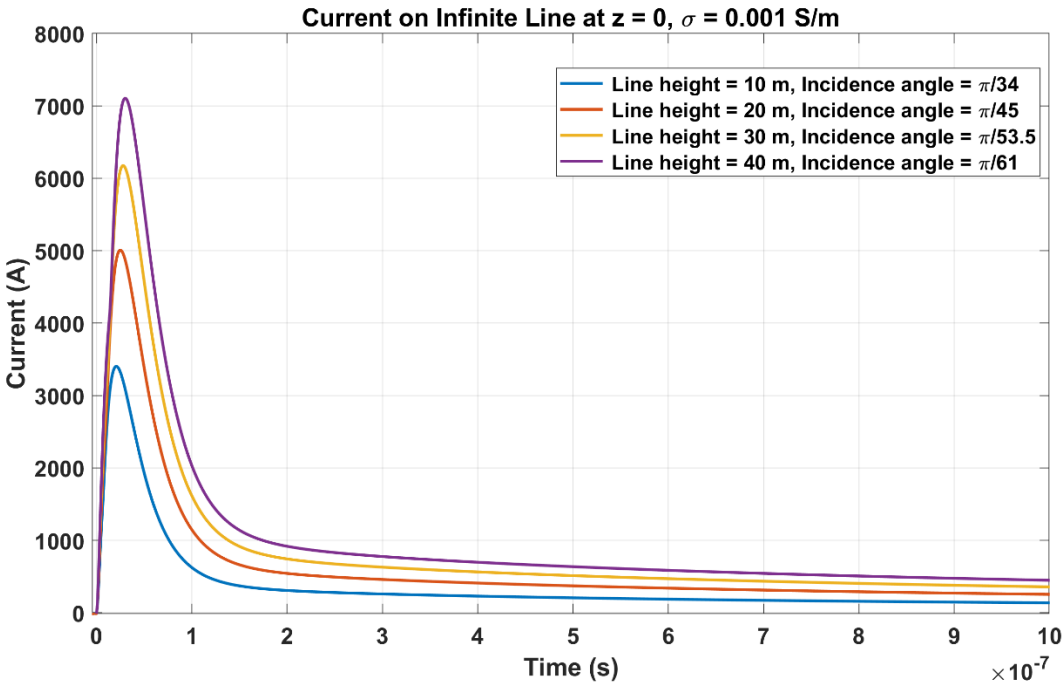

Figure 8: Time domain waveform of the current at z = 0 for the case of an infinite length line with a height of 10 m, 20 m, 30 m and 40 m, over ground with 0.001 S/m for incidence at angle of maximum coupling

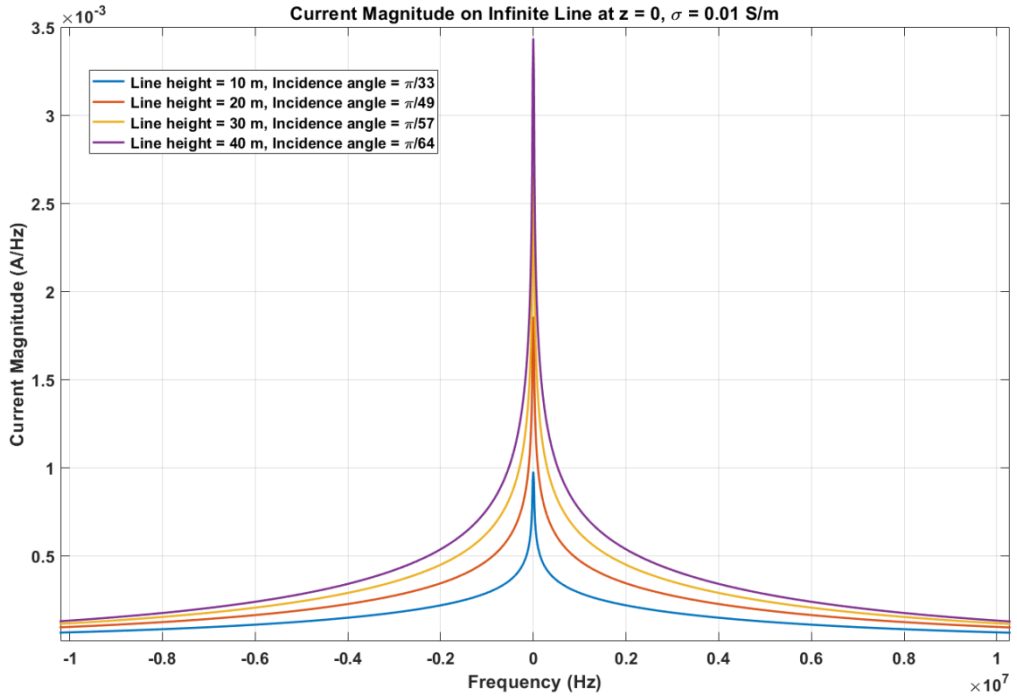

Figure 9: Frequency domain plot of the current magnitude for ground conductivity of σ = 0.01 S/m

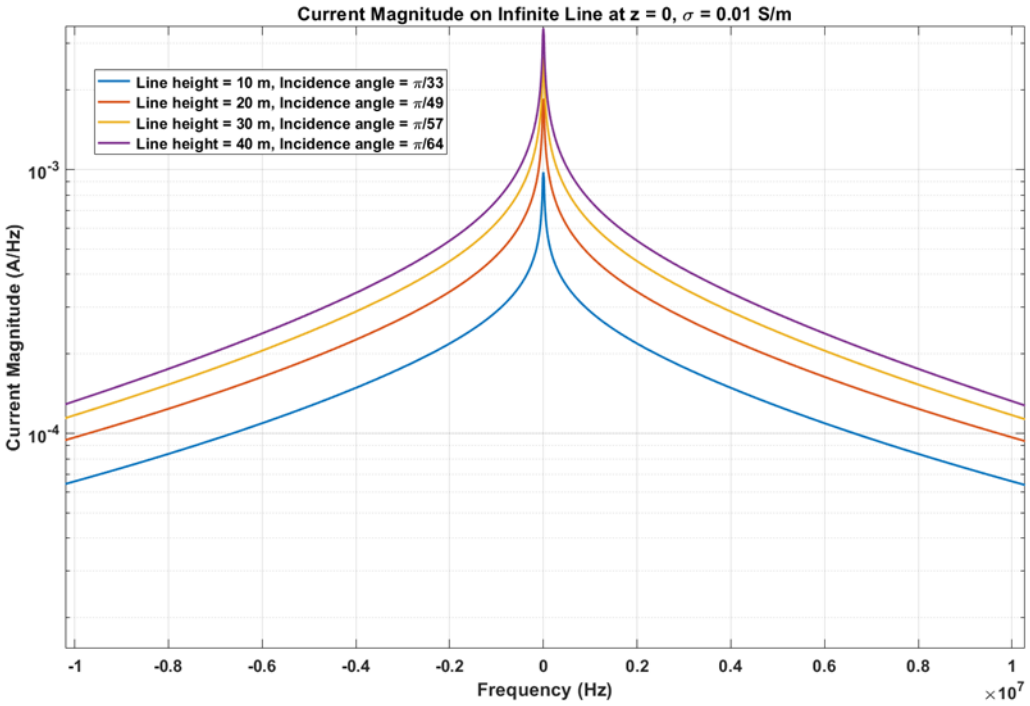

Figure 10: Frequency domain plot of the current magnitude for ground conductivity of σ = 0.01 S/m in logarithmic scale

3. METHOD USED TO EVALUATE THE ATTENUATION INDUCED BY THE TOWER LINE COUPLING

To evaluate the attenuation caused by the towers, we evaluate attenuation on an elemental building block (EBB) composed of a length of line and one tower. The EBB is shown in Figure 11. The entire transmission line can be generated by repetition of this EBB. The parameters of the building block are the length of the line segment, the height of the line, the height of the tower and the conductivity of earth. The attenuation was evaluated for the set of parameter values given in Table 2, which are representative of typical values of power line towers [11]. Figure 11 shows the elemental building block and the variable parameters.

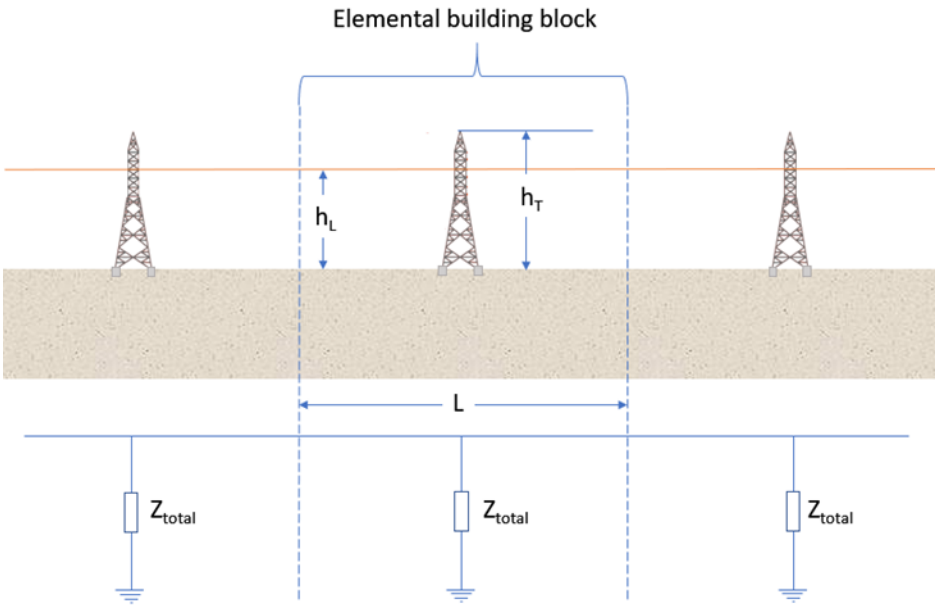

Figure 11: Elemental building block for the transmission line, which will be used to evaluate the attenuation due to the presence of the towers

Table 2: Parameters Used in the Evaluation of the Attenuation Estimations

Parameters	
Earth conductivity [S/m]	0.01
Length of line L [m]	100, 200, 300, 400
Height of tower h_T [m]	20, 30, 40
Height of line h_L [m]	10, 20, 30, 40, 50

The decay of the injected signal is evaluated in two cases, with and without tower. The tower is assumed to be at the center of the EBB, as shown in Figure 12. The attenuation produced by the tower can be evaluated from the circuit analysis of the circuit in Figure 13. This circuit includes a Norton equivalent to generate the excitation. An important quantity in the circuit analysis of the line

and the tower is the characteristic impedance of the line $Z_C = \sqrt{Z/Y}$, which corresponds to the ratio of the voltage to the current of the line. The lump circuit analysis at the point of the tower to evaluate the amount of current that goes to ground through the tower is done with the circuit in Figure 13. The ratio of the current with tower and the current without tower is given by the following formula.

$$\frac{I_{w/Tower}}{I_{wo/Tower}} = \frac{1}{1+\frac{Z_C}{2Z_{TOTAL}}} \tag{16}$$

here Z_{TOTAL} is the coupling impedance defined in Figure 2. The attenuation on an EBB is the line attenuation on a segment of length $L/2$, then the attenuation due to the coupling in Eq. (16) and finally a second line attenuation corresponding the second segment of length $L/2$, as shown in Figure 12. The line attenuation without tower is obtained from Eq. (15) under the assumption that the line attenuation is unperturbed by the presence of the tower.

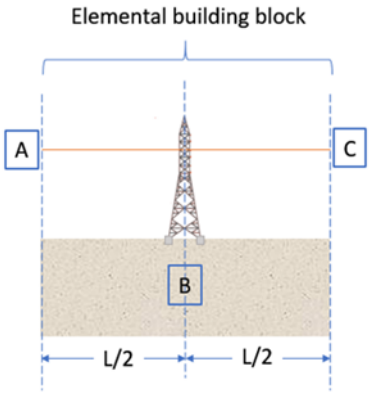

Figure 12: The current is injected at point A. The attenuation from A to C has three parts. Attenuation from A to B, attenuation at B due to the coupling to ground through the tower and the attenuation from B to C

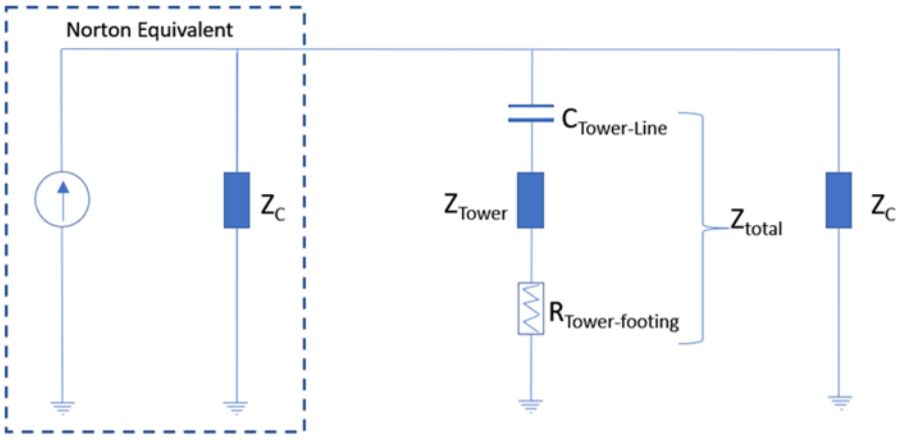

Figure 13: Equivalent circuit for the evaluation of the attenuation induced by the transmission line towers

4. ESTIMATION OF CAPACITIVE COUPLING BETWEEN LINE AND TOWER

In this section the main points of the estimation of capacitance between a line and a tower are given. Additional details are given in Appendix A. The estimation is made under the assumption of a perfect electric conductor (PEC) ground. The line and the tower are approximated by cylinders in proximity to one another at right angles, with the $z-axis$ taken to be directed along the horizontal line with $z=0$ at the position of the vertical cylinder, that represents the tower, the $y-axis$ directed vertical to the earth with $y=0$ at the surface with $x=0$ at the horizontal line and $x=\Delta$ at the position of the vertical cylinder. Assumptions about the dimensions are: line of length $2L$ and a line diameter a, with $L >> a$, tower of height h_c and tower diameter a_C, with $h_C >> a_C$. In Figure 14, the parameters used in the estimation of the capacitive coupling are shown. The approximations made here have the purpose of facilitating the analysis of the capacitance values. Improved estimates in the future can be straightforwardly incorporated into the methodology described in this report to improve the assessment of the line-tower coupling.

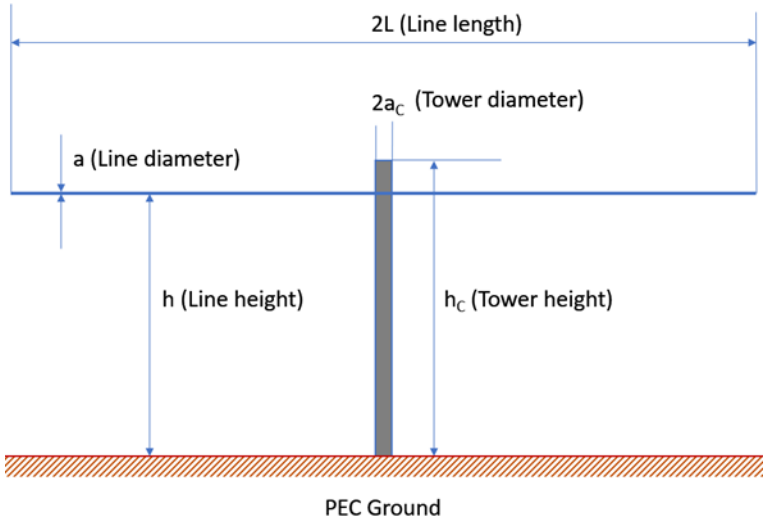

Figure 14: Line and Tower Parameters in the Evaluation of Capacitive Coupling

We estimate the electrostatic potential for the configuration of Figure 14. This is a low frequency approximation that is appropriate to estimate the coupling of the EM wave, whose spectrum, shown in Figure 9 and Figure 10, is most significant under 10MHz. The potential for the situation depicted in Figure 14 can be written as

$$\phi(x,y,z)=\frac{1}{4\pi\varepsilon_0}\lim_{L\to\infty}\left[\int_{-L}^{L}\frac{q(z')dz'}{\sqrt{x^2+(y-h)^2+(z-z')^2}}-\int_{-L}^{L}\frac{q(z')dz'}{\sqrt{x^2+(y+h)^2+(z-z')^2}}\right] \tag{17}$$

$$+\frac{1}{4\pi\varepsilon_0}\int_{-h_c}^{h_c}\frac{q_c(y')dy'}{\sqrt{(x-\Delta)^2+(y-y')^2+z^2}}$$

with $q_c(-y)=-q_c(y)$ and $h_c>h$. The charge per unit length associated with the uniform line above earth is removed to focus on the charge associated to the presence of the tower.

$$\phi(x,y,z)=\frac{1}{4\pi\varepsilon_0}\lim_{L\to\infty}\left[\int_{-L}^{L}\frac{q_0dz'}{\sqrt{x^2+(y-h)^2+(z-z')^2}}-\int_{-L}^{L}\frac{q_0dz'}{\sqrt{x^2+(y+h)^2+(z-z')^2}}-\right]$$

$$+\frac{1}{4\pi\varepsilon_0}\lim_{L\to\infty}\left[\int_{-L}^{L}\frac{(q(z')-q_0)dz'}{\sqrt{x^2+(y-h)^2+(z-z')^2}}-\int_{-L}^{L}\frac{(q(z')-q_0)dz'}{\sqrt{x^2+(y+h)^2+(z-z')^2}}-\right] \tag{18}$$

$$+\frac{1}{4\pi\varepsilon_0}\int_{-h_c}^{h_c}\frac{q_c(y')dy'}{\sqrt{(x-\Delta)^2+(y-y')^2+z^2}}$$

In this expression, the first two terms correspond to the potential of an infinite line and its image. The contribution of these two terms can be easily evaluated, for example, by evaluating the potential of a single infinite line and applying superposition. The result, which is independent of z, with $(q(z')-q_0)=\Delta q(z')$ is approximated by the expression

$$\phi(x,y,z)=\frac{1}{4\pi\varepsilon_0}\lim_{L\to\infty}\left[\int_{-L}^{L}\frac{\Delta q(z')dz'}{\sqrt{x^2+(y-h)^2+(z-z')^2}}-\int_{-L}^{L}\frac{\Delta q(z')dz'}{\sqrt{x^2+(y+h)^2+(z-z')^2}}\right] \tag{19}$$

$$+\frac{q_0}{2\pi\varepsilon_0}\ln\sqrt{\frac{x^2+(y+h)^2}{x^2+(y-h)^2}}+\frac{1}{4\pi\varepsilon_0}\int_{-h_c}^{h_c}\frac{q_c(y')dy'}{\sqrt{(x-\Delta)^2+(y-y')^2+z^2}}$$

To evaluate the capacitance, a potential difference V is assumed between the horizontal and vertical cylinder $\phi(x=0,y=h+a,z)=V, |z|<L\to\infty$ and $\phi(x=\Delta+a_c,y,z=0)=0$, with assumptions $L>>h$, $\Delta>>a_c,a$. The system of equations obtained from these boundary conditions is solved numerically to obtain q_c and Δq, as shown in the appendix, the estimates for the capacitance for various values of parameters h and h_c with $\Delta=2.4$ m are given in Table 3. The values in Table 3 were used in the attenuation calculations shown in Section 6.

Table 3: Estimated Capacitance Values for Different Line and Tower Heights

h	h_c	Capacitance
[m]	[m]	[pF]
10	20	19.2
10	30	20.4
10	40	20.8
20	30	30.7
20	40	32.8
30	40	38.5
40	50	44.5

In the following, a lump circuit analysis is used to estimate the attenuation induced by a tower. The use of lump circuit is justified by the charge distribution, which is highly concentrated near the point of closest distance between the vertical and horizontal cylinders that represent the tower and the line, respectively. The charge distribution on the line, associated to the presence of the tower (i.e. , the difference in the charge distribution with respect to charge distribution in the absence of the tower) is shown in Figure 15, where normalized charge distributions on the conductor line are given for the different cases of line and tower heights. Only positive distance is shown in Figure 15, but the same charge distribution is present on both sides of the tower along the line. As seen in the figure, the charge is highly concentrated near $z = 0$. The charge distribution on the tower for a representative example is also shown, with tower height $h_c = 40$ m and line height $h = 20$ m shown in Figure 16.

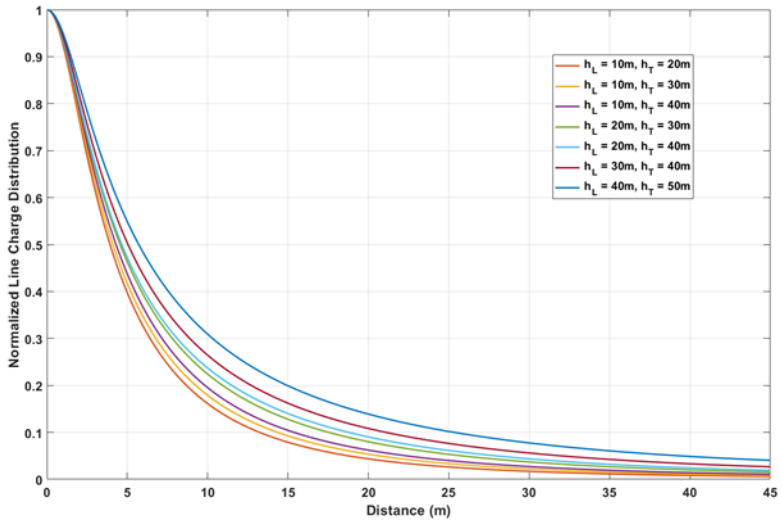

Figure 15: Normalized charge distribution on the conductor line. At zero is the tower and the charge distribution is symmetric with respect to the tower position. Only positive distance is shown in the figure

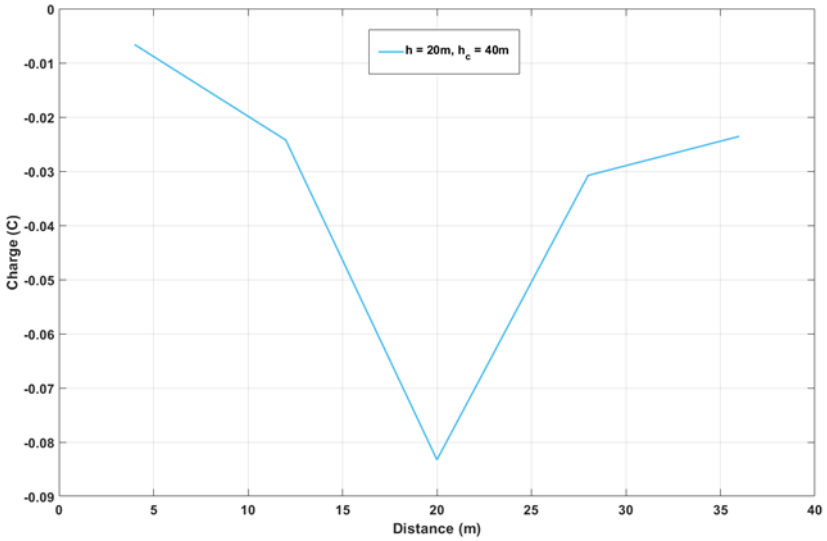

Figure 16: Charge distribution on the cylinder representing the tower

5. TOWER CHARACTERISTIC IMPEDANCE AND TOWER FOOTING RESISTANCE

As mentioned above the most significant contribution to the total impedance of the coupling Z_{Total} is the capacitance $C_{Line\text{-}Tower}$. Because the contribution of the other two parts in the total impedance is less significant, simple models have been chosen to represent these impedances. Several models have been proposed to represent the surge impedance of a transmission line tower. In 1934 Jordan proposed a first estimate [11], which was later improved by Takahashi [12]. Wagner and Hileman [13] and Sargent and Darveniza [14] also proposed expressions to represent tower surge impedance. The International Council on Large Electric Systems (CIGRE) has recommended formulas for tower characteristic impedance [15]. In the case of a cylindrical conductor the expressions proposed are:

$$Z_S = 60\ \ln\left(\frac{h}{r_C}\right)\ \Omega \quad \text{(CIGRE [7])} \tag{20}$$

$$Z_S = 60\ln\left(\sqrt{2}\,\frac{2h}{r_C}\right) - 60\ \Omega \quad \text{(Sargent and Darveniza [14])} \tag{21}$$

Recently, Gutierrez et al. proposed a new methodology to derive the tower impedance based on the use of transmission line segments [16]. For the case of a single vertical conductor over conductive ground, the field distribution of the conductor and its image can be approximated by that of a bi-conical antenna, which leads to the following expression for the surge impedance

$$Z_S = \frac{1}{2\pi}\sqrt{\frac{\mu}{\varepsilon}}\ln\left[\frac{h+\sqrt{h+r_C}}{r_C}\right] + \frac{1}{2\pi}\sqrt{\frac{\mu}{\varepsilon}}\ln\left[\frac{(h+p)+\sqrt{(h+p)^2+{r_C}^2}}{h+\sqrt{h^2+{r_C}^2}}\right] \tag{22}$$

where p is the complex skin depth $p = 1/\sqrt{j\omega\mu_E\sigma_E}$ that accounts for the ground conductivity losses [17], [18], with μ_E and σ_E magnetic permeability and electrical conductivity of the soil. In the above expressions h is the height of the cylinder that represents the tower and r_C its radius, as shown in Figure 15. Any of the expressions above (20)-(22), give similar results for the attenuations. In the results for the attenuation caused by the tower given below, the expression in Eq. (22) was used. This impedance corresponds to the characteristic impedance of the tower represented as a transmission line with the footing resistance as a termination load of the line.

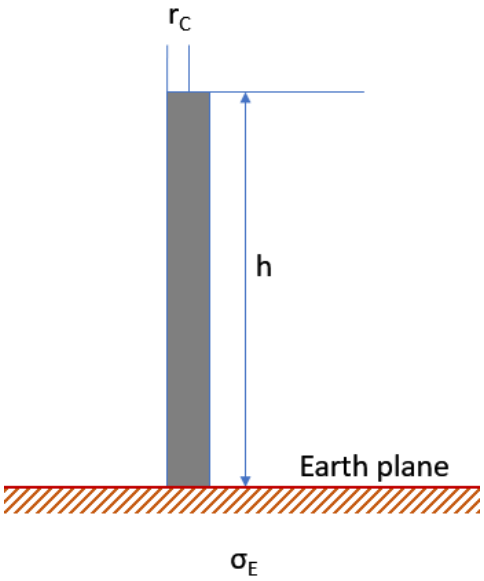

Figure 17: Cylinder that represents the tower in the calculation of the tower surge impedance

The tower footing impedance in lightning strike studies is represented by a non-linear resistance, where the non-linearity is caused by the ionization of the ground [19].

$$R_{Tower\text{-}footing} = \frac{R_0}{\sqrt{1 + I/I_g}} \tag{23}$$

In our case, it is assumed that the current is not enough to trigger the non-linear effect $R_T = R_0$, with the value of $R_0 = 12.5\ \Omega$, a high frequency approximation for vertical ground rod divided by 4 to account for the 4 supports of a typical tower [20]. This value has been included, but the result for the maximum current would not be affected if this value was equal to zero, because the E1-HEMP induced excitation, with IEC61000-2-9, is very narrow in time, with the maximum current occurring at approximately 25 ns, which is much shorter than the time require for the first reflection from the tower base to arrive. This can be seen in Figure 18, where the reflection from the tower footing, due to the delay, does not affect the value of the maximum current. The total impedance of the combined capacitive coupling between line and tower and the characteristic impedance of the tower with the termination load of the footing resistance is

$$Z_{Total} = \frac{1}{j\omega C_{Line\text{-}Tower}} + Z_{Tower}\left(\frac{R_{Tower\text{-}footing} + jZ_{Tower}\tan(kL)}{Z_{Tower} + jR_{Tower\text{-}footing}\tan(kL)}\right) \tag{24}$$

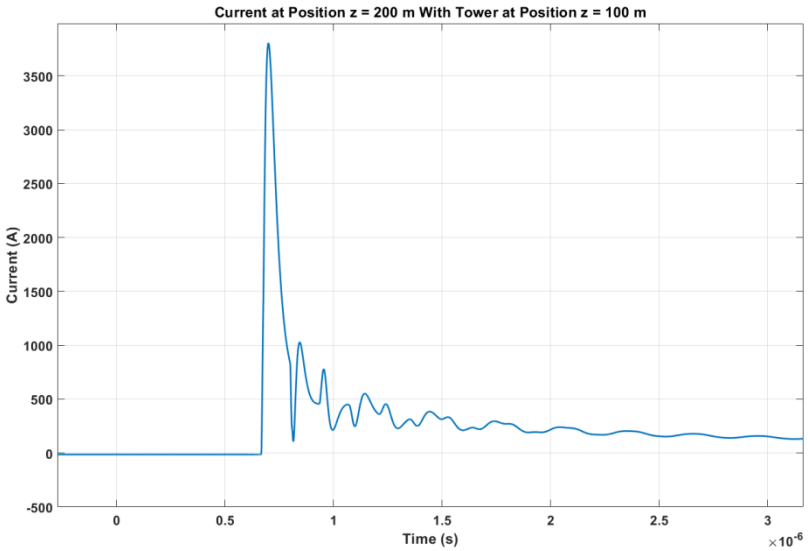

Figure 18: Reflection from tower footing with tower height = 30 m and line height = 20 m

6. ATTENUATION RESULTS FOR THE PARAMETERS IN TABLE 2

In Tables 4-10, the results for the attenuation at the end of the elemental building block are presented, i.e. at position C in Fig. 6 for the case of $\sigma = 0.01$ S/m. In Tables 11-17, the results for the attenuation for the case of $\sigma = 0.001$ S/m are presented. The angle of maximum coupling θ used in the evaluation, is given in each table. In each case, both the values of attenuation with and without the tower are given. The results are all less than one because the attenuation is given as a per one reduction of the initial amplitude. Tower distance in tables refers to the distance between towers. The relative significance is best assessed by comparing to the attenuation due to the losses in the ground.

Table 4: Tower Height = 20 m, Line Height = 10 m, $\theta = \pi/33$, $\sigma = 0.01$ S/m

Tower distance	100 m	200 m	300 m	400 m
wo/towers	0.9100	0.8297	0.7578	0.6940
w/towers	0.8473	0.7740	0.7080	0.6481

Table 5: Tower Height = 30 m, Line Height = 10 m, $\theta = \pi/33$, $\sigma = 0.01$ S/m

Tower distance	100 m	200 m	300 m	400 m
wo/towers	0.9100	0.8297	0.7578	0.6940
w/towers	0.8390	0.7666	0.7014	0.6423

Table 6: Tower Height = 40 m, Line Height = 10 m, $\theta = \pi/33$, $\sigma = 0.01$ S/m

Tower distance	100 m	200 m	300 m	400 m
wo/towers	0.9100	0.8297	0.7578	0.6940
w/towers	0.8346	0.7627	0.6979	0.6392

Table 7: Tower Height = 30 m, Line Height = 20 m, $\theta = \pi/49$, $\sigma = 0.01$ S/m

Tower distance	100 m	200 m	300 m	400 m
wo/towers	0.9581	0.9182	0.8802	0.8443
w/towers	0.8327	0.8001	0.7689	0.7388

Table 8: Tower Height = 40 m, Line Height = 20 m, $\theta = \pi/49$, $\sigma = 0.01$ S/m

Tower distance	100 m	200 m	300 m	400 m
wo/towers	0.9581	0.9182	0.8802	0.8443
w/towers	0.8210	0.7888	0.7580	0.7287

Table 9: Tower Height = 40 m, Line Height = 30 m, θ = π/57, σ = 0.01 S/m

Tower distance	100 m	200 m	300 m	400 m
wo/towers	0.9738	0.9483	0.9238	0.9000
w/towers	0.8205	0.8006	0.7812	0.7623

Table 10: Tower Height = 50 m, Line Height = 40 m, θ = π/64, σ = 0.01 S/m

Tower distance	100 m	200 m	300 m	400 m
wo/towers	0.9812	0.9629	0.9449	0.9274
w/towers	0.8095	0.7954	0.7818	0.7682

Table 11: Tower Height = 20 m, Line Height = 10 m, θ = π/34, σ = 0.001 S/m

Tower distance	100 m	200 m	300 m	400 m
wo/towers	0.8827	0.7792	0.6878	0.6070
w/towers	0.8021	0.7082	0.6253	0.5527

Table 12: Tower Height = 30 m, Line Height = 10 m, θ = π/34, σ = 0.001 S/m

Tower distance	100 m	200 m	300 m	400 m
wo/towers	0.8827	0.7792	0.6878	0.6070
w/towers	0.7929	0.6999	0.6183	0.5460

Table 13: Tower Height = 40 m, Line Height = 10 m, θ = π/34, σ = 0.001 S/m

Tower distance	100 m	200 m	300 m	400 m
wo/towers	0.8827	0.7792	0.6878	0.6070
w/towers	0.7882	0.6961	0.6149	0.5430

Table 14: Tower Height = 30 m, Line Height = 20 m, θ = π/45, σ = 0.001 S/m

Tower distance	100 m	200 m	300 m	400 m
wo/towers	0.9441	0.8914	0.8419	0.7947
w/towers	0.8032	0.7590	0.7169	0.6775

Table 15: Tower Height = 40 m, Line Height = 20 m, θ = π/45, σ = 0.001 S/m

Tower distance	100 m	200 m	300 m	400 m
wo/towers	0.9441	0.8914	0.8419	0.7947
w/towers	0.7914	0.7476	0.7063	0.6675

Table 16: Tower Height = 40 m, Line Height = 30 m, θ = π/53.5, σ = 0.001 S/m

Tower distance	100 m	200 m	300 m	400 m
wo/towers	0.9637	0.9292	0.8959	0.8635
w/towers	0.7897	0.7529	0.7346	0.7083

Table 17: Tower Height = 50 m, Line Height = 40 m, θ = π/61, σ = 0.001 S/m

Tower distance	100 m	200 m	300 m	400 m
wo/towers	0.9737	0.9478	0.9230	0.8985
w/towers	0.7774	0.7571	0.7373	0.7181

In Figs. 19-22 the same data is presented in graphical form. Fig. 19 shows the results for a line height of 10 m and multiple tower heights. The plot shows the case without tower in blue, and three cases with tower heights of 20 m, 30 m and 40 m. Clearly for a fix line height, variations in tower height have a relatively small effect on the attenuation.

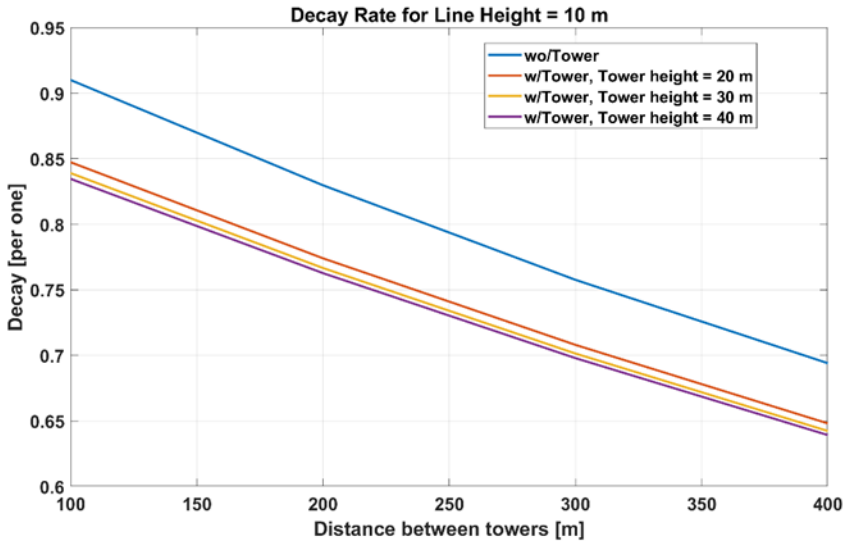

Figure 19: For a line height of 10 m the decays as functions of distance between towers is given for cases without tower, shown in blue, and three cases with tower, with tower heights of 20 m, 30 m and 40 m

Fig. 20 shows the results for the case of a line height of 20 m. The plot shows the case without tower in blue and two cases with tower heights of 30 m and 40 m.

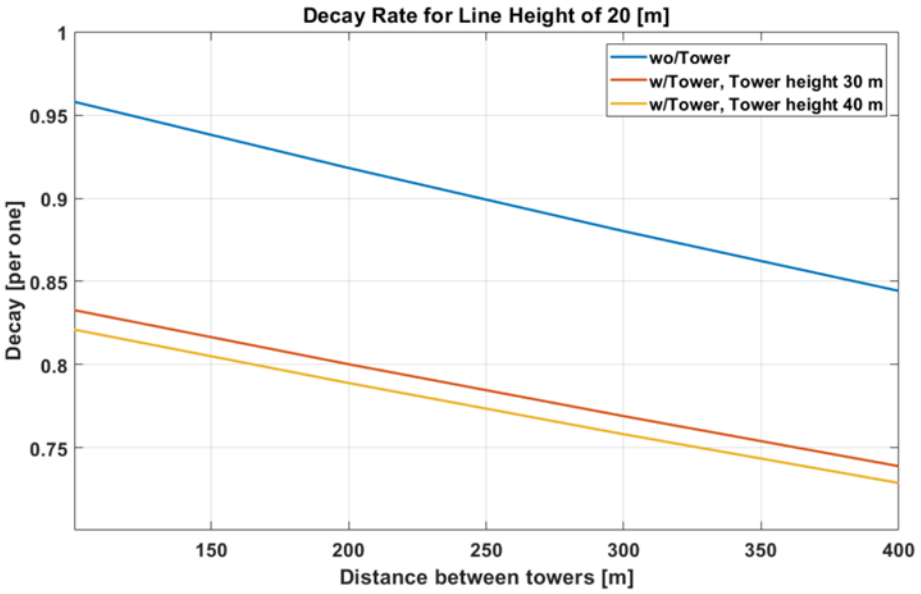

Figure 20: For a line height of 20m the decay as a function of distance between towers is shown for the cases without tower, shown in blue, and two cases with towers, with tower heights of 30 m and 40 m

Fig. 21 shows the results for the case of a line height of 30 m. The plot shows the case without tower in blue and a case with tower height of 40 m.

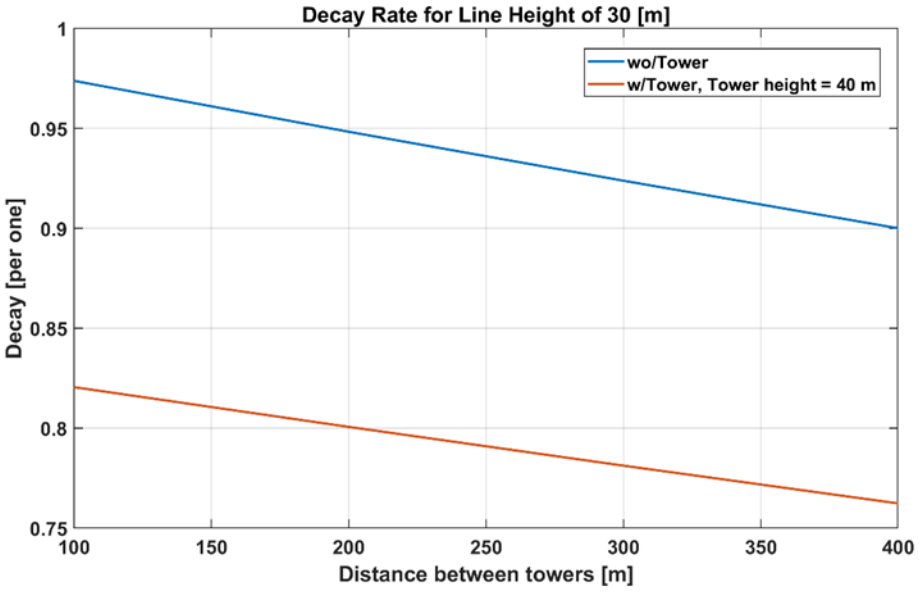

Figure 21: For a line height of 30 m the decay as a function of distance between towers is shown for the case without tower in blue and the case of a tower height of 40 m

In Fig. 22 the results for a line height of 40 m are shown. The plot shows the case without tower in blue and the case with tower height of 50 m.

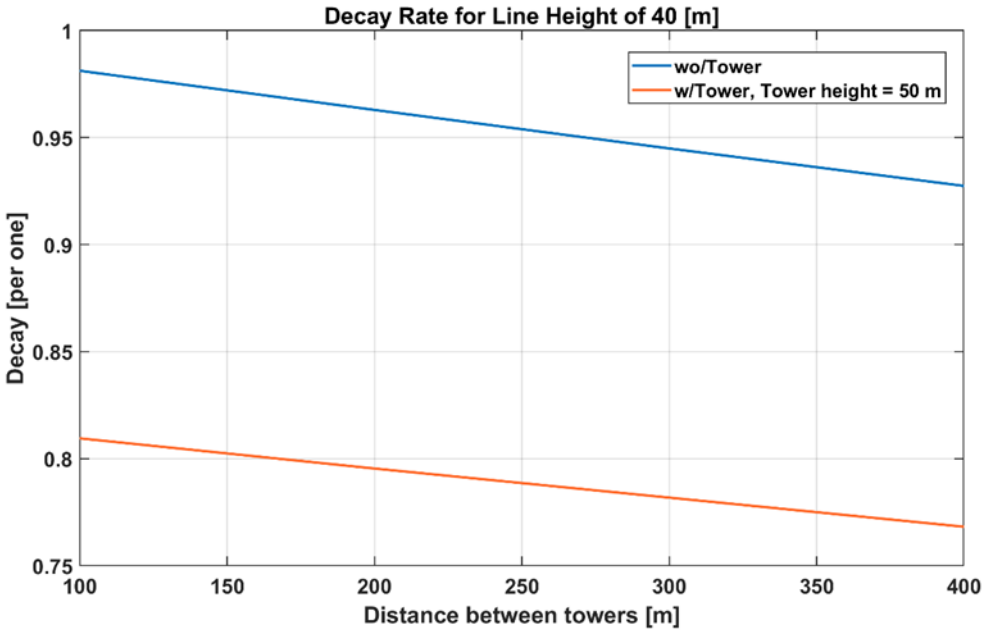

Figure 22: For a line of 40 m height the decay as a function of the distance between towers is shown for the case without tower in blue and for the case of tower height of 50 m

7. CONCLUSIONS

As can be seen in the tables and plots, the attenuation due to the line-tower coupling varies from approximately 5% for a line height of 10 m with a tower of 20 m, to a 20% for a line height of 40 m with a tower of 50 m. The effect increases as the line height increases, which is opposite to the ground losses that decrease as line height increases. The amount of attenuation can be defined as 1 – (number on the table). The ratio of the amount of attenuation with tower divided by the amount of attenuation without tower is always larger than one varies between approximately 1.5 and 10, with 1.5 and 10 corresponding to a line height of 10 m and 40 m, respectively. This means that the attenuation associated with the line tower coupling can be 10 times larger than the attenuation due to the losses in the ground, which means that the line tower coupling effect can be very significant. Another conclusion from the results, see Fig. 19 for example, is that for a fix line height the variation associated with changes in tower height is relatively small.

REFERENCES

[1] Carson, J. R., “Wave propagation in overhead wires with ground return," The Bell System Technical Journal, Vol. 5, 539-554, 1926.

[2] Sunde, E. D., Earth Conduction Effects in Transmission Systems, Dover, New York, 1967.

[3] Wait, J. R., “Theory of wave propagation along a thin wire parallel to an interface," Radio Science, Vol. 7, 675{679, 1972.

[4] Wait, J. R., “Tutorial note on the general transmission line theory for a thin wire above the ground," IEEE Transactions on Electromagnetic Compatibility, Vol. 33, 65-67, 1991.

[5] Campione, S., L. K. Warne, L. I. Basilio, C. D. Turner, K. L. Cartwright, and K. C. Chen, “Electromagnetic pulse excitation of finite- and infinitely-long lossy conductors over a lossy ground plane," Journal of Electromagnetic Waves and Applications, Vol. 31, 209-224, 2017.

[6] Warne, L. K. and K. C. Chen, “Long line coupling models," Sandia National Laboratories Report, Vol. SAND2004-0872, Albuquerque, NM, 2004.

[7] Campione, S., L. L.K. Warne, R.L. Schiek, and L.I. Basilio, “Electromagnetic pulse excitation of finite-long dissipative conductors over a conducting ground plane in the frequency domain,” SANDIA Report SAND2017-10078, September 2017.

[8] International Standard – Electromagnetics Compatibility, IEC 61000-2-9, 1966.

[9] Campione, S., L. K. Warne, L. I. Basilio, C. D. Turner, K. L. Cartwright, and K. C. Chen, “Electromagnetic Pulse Excitation of Finite- and Infitely-Long Lossy Conductors Over a Lossy Ground Plane,” Journal of Electromagnetic Waves and Applications, Vol. 31, 209-224, 2017.

[10] S. Campione, L. K. Warne, M. Halligan, O. Lavrova, and L. San Martin, "Decay Length Estimation of Single-, Two-, and Three-Wire Systems Above Ground Under HEMP Excitation," Progress In Electromagnetics Research B, Vol. 84, 23-42, 2019. doi:10.2528/PIERB19010803.

[11] EPRI, “Transmission line reference book”, Second edition (revised), 537.12 Tr69 1982.

[12] C. A. Jordan “Lightning computations for transmission lines with overhead ground wires, Part II,” Gen. Electr. Rev, vol,37, no pp.180-186,1934.

[13] H. Takahashi, “Confirmation of the error of Jordan’s formula on tower surge impedance,” Trans. Inst. Elect. Eng. Jpn., vol. 114-B, pp. 112-113, 1994 (in Japanese).

[14] C. F. Wagner and A. R. Hileman, “A new approach to the calculation of the lightning performance of transmission line III-A simplified method: Stroke to tower,” AIEEE Trans. Part III, vol. 79, pp. 589-603, Oct. 1990.

[15] M. A. Sargent and M. Darveniza, “Tower surge impedance” IEEE Trans. Power App. Syst., vol. PAS-88, no. 5, pp. 680-687, May 1969.

[16] S. Visacro and F. H. Silveira, “Guide to procedures for estimating lightning performance of transmission lines,” CIGRE SC33-WG01, Tech. Brochure, Oct. 1991.

[17] J. A. Gutierrez, R., J. L. Naredo, J. L. Bermudez, M. Paolone, C. A. Nucci, and F. Rachidi, “Nonuniform Transmission Tower Model for Lightning Transient Studies,” IEEE Transactions on Power Delivery, vol 19, no. 2, April 2004.

[18] C. Gary, Approche Complete de la propagation multifilaire en haute frequence par utilization des matrices complexes, in EdF Bulletin de la Direction des Etudes et Recherches, no. 3/4, ser. B, pp. 5–20, 1976.

[19] A. Semlyen and A. Deri, “Time domain modeling of frequency dependent three-phase transmission line impedance,” IEEE Trans. Power App. Syst., vol. PAS-104, pp. 1549–1555, June 1985.

[20]] Juan A. Martinez, and Ferley Castro-Aranda, “Tower Modeling for Lightning Analysis of Overhead Transmission Lines”, IEEE Power Engineering Society General Meeting, San Francisco, Ca, USA, 2005.

[21] L. Grcev and M. Popov, “On high-frequency circuit equivalents of a vertical ground rod,” IEEE Trans. Power Del., vol. 20, no. 2, pp. 1598–1603, Apr. 2005.

APPENDIX A. EVALUATION OF THE COUPLING CAPACITANCE BETWEEN TOWER AND LINE

The potential of the PEC cylinders representing the line and the tower above PEC ground can be approximated as:

$$\phi(x,y,z)=\frac{1}{4\pi\varepsilon_0}\lim_{L\to\infty}\left[\int_{-L}^{L}\frac{\Delta q(z')dz'}{\sqrt{x^2+(y-h)^2+(z-z')^2}}-\int_{-L}^{L}\frac{\Delta q(z')dz'}{\sqrt{x^2+(y+h)^2+(z-z')^2}}\right]$$

$$+\frac{q_0}{2\pi\varepsilon_0}\ln\sqrt{\frac{x^2+(y+h)^2}{x^2+(y-h)^2}}+\frac{1}{4\pi\varepsilon_0}\int_{-h_c}^{h_c}\frac{q_c(y')dy'}{\sqrt{(x-\Delta)^2+(y-y')^2+z^2}} \qquad \text{(A.1)}$$

By imposing the boundary conditions $\phi(x=0,y=h+a,z)=V, |z|<L\to\infty$ and $\phi(x=\Delta+a_c,y,z=0)=V_c$, with the assumption $L>>h$, $\Delta>>a_c,a$, equations that relate charge and potential are obtained. From these equations the capacitance can be derived. The unknowns Δq and q_c are discretized as follows:

$\Delta q(z)=\sum_{n=0}^{N}\frac{1}{2}\varepsilon_n\Delta q_n\left[p_n(z)+p_n(-z)\right]$ with $p_n(z)=1$ if $-\Delta_h/2<z-z_n<\Delta_h/2$ and $p_n(z)=0$ otherwise,

$q_c(y)=\sum_{m=1}^{M}q_{cm}\left[p_m(y)-p_m(-y)\right]$ with $p_m(y)=1$ if $-\Delta_v/2<y-y_m<\Delta_v/2$ and $p_m(y)=0$ otherwise .With $z_n=n\Delta_h$, $z_N=L-\Delta_h/2$ and $(2N+1)\Delta_h=2L$, and

$y_m=m\Delta_v-\Delta_v/2$ and $M\Delta_v=h_c$. The symbol ε_n above is the Neumann symbol, which is equal to 1 for $n=0$ and 2 for all other cases. By substituting the discrete representations of Δq and q_c into Eq. (A.1) and considering that $V=\frac{q_0}{2\pi\varepsilon_0}\ln\sqrt{\frac{x^2+(y+h)^2}{x^2+(y-h)^2}}$,

$$0=\sum_{n'=0}^{N}\frac{1}{2}\varepsilon_{n'}\Delta q_{n'}\left[\int_{-L}^{L}\frac{p_{n'}(z')+p_{n'}(-z')}{\sqrt{a^2+(z_n-z')^2}}dz'-\int_{-L}^{L}\frac{p_{n'}(z')+p_{n'}(-z')}{\sqrt{(2h)^2+(z_n-z')^2}}dz'\right]+\sum_{m'=1}^{M}q_{cm'}\int_{-h_c}^{h_c}\frac{p_{m'}(y')-p_{m'}(-y')}{\sqrt{\Delta^2+z_n^2+(h-y')^2}}dy' \qquad \text{(A.2)}$$

$$v_c=\sum_{n'=0}^{N}\frac{1}{2}\varepsilon_{n'}\Delta q_{n'}\left[\int_{-L}^{L}\frac{p_{n'}(z')+p_{n'}(-z')}{\sqrt{\Delta^2+(y_m-h)^2+z'^2}}dz'-\int_{-L}^{L}\frac{p_{n'}(z')+p_{n'}(-z')}{\sqrt{\Delta^2+(z_n-z')^2}}dz'\right]$$

$$+\frac{1}{\ln(2h/a)}\ln\sqrt{\frac{(\Delta+a_c)^2+(y_{m'}+h)^2}{(\Delta+a_c)^2+(y_{m'}-h)^2}}+\sum_{m'=1}^{M}q_{cm'}\int_{-h_c}^{h_c}\frac{p_{m'}(y')-p_{m'}(-y')}{\sqrt{a_c^2+z_n^2+(h-y')^2}}dy' \qquad \text{(A.3)}$$

The integrations can be done one the intervals where $p_n(z)$ and $p_m(y)$ are different from zero. Thus,

$$0=\sum_{n'=0}^{N}\frac{1}{2}\varepsilon_{n'}\Delta q_{n'}\left[\int_{-\Delta_h/2}^{\Delta_h/2}\frac{dz'}{\sqrt{a^2+(z_n-z_{n'}-z')^2}}-\int_{-\Delta_h/2}^{\Delta_h/2}\frac{dz'}{\sqrt{a^2+(z_n-z_{n'}-z')^2}}\right.$$

$$-\int_{-\Delta_h/2}^{\Delta_h/2}\frac{dz'}{\sqrt{(2h)^2+(z_n-z_{n'}-z')^2}}-\int_{-\Delta_h/2}^{\Delta_h/2}\frac{dz'}{\sqrt{(2h)^2+(z_n-z_{n'}-z')^2}}\Bigg]$$

$$+\sum_{m'=1}^{M}q_{cm'}\left[\int_{-\Delta_v/2}^{\Delta_v/2}\frac{dy'}{\sqrt{\Delta^2+z_n^2+(h-y_{m'}-y')^2}}dy'-\int_{-\Delta_v/2}^{\Delta_v/2}\frac{dy'}{\sqrt{\Delta^2+z_n^2+(h+y_{m'}-y')^2}}dy'\right] \quad (A.4)$$

$$v_c=\sum_{n'=0}^{N}\varepsilon_{n'}\Delta q_{n'}\left[\int_{-\Delta_h/2}^{\Delta_h/2}\frac{dz'}{\sqrt{\Delta^2+(y_m-h)^2+(z_{n'}-z')^2}}-\int_{-\Delta_h/2}^{\Delta_h/2}\frac{dz'}{\sqrt{\Delta^2+(y_m+h)^2+(z_{n'}-z')^2}}\right] \quad (A.5)$$

$$+\frac{1}{\ln(2h/a)}\ln\sqrt{\frac{(\Delta+a_c)^2+(y_m+h)^2}{(\Delta+a_c)^2+(y_m-h)^2}}+\sum_{m'=1}^{M}q_{cm'}\left[\int_{-\Delta_v/2}^{\Delta_v/2}\frac{dy'}{\sqrt{a_c^2+(y_m-y_{m'}-y')^2}}-\int_{-\Delta_v/2}^{\Delta_v/2}\frac{dy'}{\sqrt{a_c^2+(y_m+y_{m'}-y')^2}}\right]$$

By appropriate change of variables, some of the integrals can be rewritten as:

$$0=\sum_{n'=0}^{N}\frac{1}{2}\varepsilon_{n'}\Delta q_{n'}\left[\int_{z_n-z_{n'}-\Delta_h/2}^{z_n-z_{n'}+\Delta_h/2}\frac{du}{\sqrt{a^2+u^2}}+\int_{z_n+z_{n'}-\Delta_h/2}^{z_n+z_{n'}+\Delta_h/2}\frac{du}{\sqrt{a^2+u^2}}-\int_{z_n-z_{n'}-\Delta_h/2}^{z_n-z_{n'}+\Delta_h/2}\frac{du}{\sqrt{(2h)^2+u^2}}-\int_{z_n+z_{n'}-\Delta_h/2}^{z_n+z_{n'}+\Delta_h/2}\frac{du}{\sqrt{(2h)^2+u^2}}\right] \quad (A.6)$$

$$+\sum_{m'=1}^{M}q_{cm'}\left[\int_{h-y_{m'}-\Delta_v/2}^{h-y_{m'}+\Delta_v/2}\frac{du}{\sqrt{\Delta^2+z_n^2+u^2}}dy'-\int_{h+y_{m'}-\Delta_v/2}^{h+y_{m'}+\Delta_v/2}\frac{du}{\sqrt{\Delta^2+z_n^2+u^2}}dy'\right]$$

$$v_c=\sum_{n'=0}^{N}\varepsilon_{n'}\Delta q_{n'}\left[\int_{z_{n'}-\Delta_h/2}^{z_{n'}+\Delta_h/2}\frac{du}{\sqrt{\Delta^2+(y_m-h)^2+u^2}}-\int_{z_{n'}-\Delta_h/2}^{z_{n'}+\Delta_h/2}\frac{du}{\sqrt{\Delta^2+(y_m+h)^2+u^2}}\right] \quad (A.7)$$

$$+\frac{1}{\ln(2h/a)}\ln\sqrt{\frac{(\Delta+a_c)^2+(y_m+h)^2}{(\Delta+a_c)^2+(y_m-h)^2}}+\sum_{m'=1}^{M}q_{cm'}\left[\int_{y_m-y_{m'}-\Delta_v/2}^{y_m-y_{m'}+\Delta_v/2}\frac{du}{\sqrt{a_c^2+u^2}}-\int_{y_m+y_{m'}-\Delta_v/2}^{y_m+y_{m'}+\Delta_v/2}\frac{du}{\sqrt{a_c^2+u^2}}\right]$$

Then, by using the identity $\int\frac{du}{\sqrt{u^2+a^2}}=\ln(u+\sqrt{u^2+a^2})$,

$$0=\sum_{n'=0}^{N}\frac{1}{2}\varepsilon_{n'}\Delta q_{n'}\left[\ln\left\{\frac{z_n-z_{n'}+\Delta_h/2+\sqrt{(z_n-z_{n'}+\Delta_h/2)^2+a^2}}{z_n-z_{n'}-\Delta_h/2+\sqrt{(z_n-z_{n'}-\Delta_h/2)^2+a^2}}\frac{z_n-z_{n'}-\Delta_h/2+\sqrt{(z_n-z_{n'}-\Delta_h/2)^2+(2h)^2}}{z_n-z_{n'}+\Delta_h/2+\sqrt{(z_n-z_{n'}+\Delta_h/2)^2+(2h)^2}}\right\}\right.$$

$$\left.\ln\left\{\frac{z_n+z_{n'}+\Delta_h/2+\sqrt{(z_n+z_{n'}+\Delta_h/2)^2+a^2}}{z_n+z_{n'}-\Delta_h/2+\sqrt{(z_n+z_{n'}-\Delta_h/2)^2+a^2}}\frac{z_n+z_{n'}-\Delta_h/2+\sqrt{(z_n+z_{n'}-\Delta_h/2)^2+(2h)^2}}{z_n+z_{n'}+\Delta_h/2+\sqrt{(z_n+z_{n'}+\Delta_h/2)^2+(2h)^2}}\right\}\right]$$

$$\sum_{m'=1}^{M}q_{cm'}\ln\left\{\frac{h-y_{m'}+\Delta_v/2+\sqrt{(h-y_{m'}+\Delta_v/2)^2+\Delta^2+z_n^2}}{h-y_{m'}-\Delta_v/2+\sqrt{(h-y_{m'}-\Delta_v/2)^2+\Delta^2+z_n^2}}\frac{h-y_{m'}-\Delta_v/2+\sqrt{(h-y_{m'}-\Delta_v/2)^2+\Delta^2+z_n^2}}{h-y_{m'}+\Delta_v/2+\sqrt{(h-y_{m'}+\Delta_v/2)^2+\Delta^2+z_n^2}}\right\} \quad (A.8)$$

$$v_c=\sum_{n'=0}^{N}\varepsilon_{n'}\Delta q_{n'}\ln\left\{\frac{z_{n'}+\Delta_h/2+\sqrt{(z_{n'}+\Delta_h/2)^2+\Delta^2+(y_m-h)^2}}{z_{n'}-\Delta_h/2+\sqrt{(z_{n'}-\Delta_h/2)^2+\Delta^2+(y_m-h)^2}}\frac{z_{n'}-\Delta_h/2+\sqrt{(z_{n'}-\Delta_h/2)^2+\Delta^2+(y_m+h)^2}}{z_{n'}+\Delta_h/2+\sqrt{(z_{n'}+\Delta_h/2)^2+\Delta^2+(y_m+h)^2}}\right\}$$

$$+\frac{1}{\ln(2h/a)}\ln\sqrt{\frac{(\Delta+a_c)^2+(y_m+h)^2}{(\Delta+a_c)^2+(y_m-h)^2}}$$

$$+\sum_{n'=0}^{N} q_{cm'}\ln\left\{\frac{y_m-y_{m'}+\Delta_v/2+\sqrt{(y_m-y_{m'}+\Delta_v/2)^2+a_c^2}}{y_m-y_{m'}-\Delta_v/2+\sqrt{(y_m-y_{m'}-\Delta_v/2)^2+a_c^2}}\,\frac{y_m+y_{m'}-\Delta_v/2+\sqrt{(y_m+y_{m'}-\Delta_v/2)^2+a_c^2}}{y_m+y_{m'}+\Delta_v/2+\sqrt{(y_m+y_{m'}+\Delta_v/2)^2+a_c^2}}\right\} \quad \text{(A.9)}$$

with $\Delta q=\Delta_h\sum_{n=0}^{N}\varepsilon_n\Delta q_n$ and $q_c=\Delta_v\sum_{m=1}^{M}q_{cm}$ a capacitance matrix can be derived of the form

$$\begin{pmatrix}\Delta q\\ q_c\end{pmatrix}=\begin{pmatrix}C_{11} & C_{12}\\ C_{21} & C_{22}\end{pmatrix}\begin{pmatrix}V\\ V_c\end{pmatrix} \quad \text{(A.10)}$$

from where the capacitance can be evaluated by making $V_c=0$, so that $\Delta q=C_{11}V$ and the capacitance associated to the change in charge due to the presence of the tower Δq is C_{11}.

DISTRIBUTION

Email—Internal

Name	Org.	Sandia Email Address
Luis San Martin	01352	lsanmar@sandia.gov
Ross Guttromson	08812	rguttro@sandia.gov
Matthew Halligan	01353	mhallig@sandia.gov
Craig Lawton	08141	crlawto@sandia.gov
Charles Hanley	08810	cjhanle@sandia.gov
William Langston	01352	wllangs@sandia.gov
Technical Library	01977	sanddocs@sandia.gov

This page left blank

This page left blank

Sandia National Laboratories

Sandia National Laboratories is a multimission laboratory managed and operated by National Technology & Engineering Solutions of Sandia LLC, a wholly owned subsidiary of Honeywell International Inc. for the U.S. Department of Energy's National Nuclear Security Administration under contract DE-NA0003525.